nature
structural &
molecular biology

Sec15 interacts with Rab11 via a novel domain and affects Rab11 localization *in vivo*

Shuya Wu[1], Sunil Q Mehta[2], Franck Pichaud[3], Hugo J Bellen[2,4,5] & Florante A Quiocho[1]

Sec15, a component of the exocyst, recognizes vesicle-associated Rab GTPases, helps target transport vesicles to the budding sites in yeast and is thought to recruit other exocyst proteins. Here we report the characterization of a 35-kDa fragment that comprises most of the C-terminal half of *Drosophila melanogaster* Sec15. This C-terminal domain was found to bind a subset of Rab GTPases, especially Rab11, in a GTP-dependent manner. We also provide evidence that in fly photoreceptors Sec15 colocalizes with Rab11 and that loss of Sec15 affects rhabdomere morphology. Determination of the 2.5-Å crystal structure of the C-terminal domain revealed a novel fold consisting of ten α-helices equally distributed between two subdomains (N and C subdomains). We show that the C subdomain, mainly via a single helix, is sufficient for Rab binding.

During exocytosis, membrane-bound secretory vesicles fuse with the plasma membrane. This process is important for membrane expansion, cell growth, establishment of polarity, neurotransmitter release, hormone release, delivery of specific proteins to the cell membrane and other processes. Numerous proteins have been implicated in the transport, docking, priming and fusion of vesicles. One complex of proteins, named the exocyst, is important for exocytosis in yeast and is required for targeting and docking vesicles to specific membrane sites during budding[1–3].

The yeast exocyst contains six *sec* gene products—Sec3p, Sec5p, Sec6p, Sec8p, Sec10p, Sec15p—and two additional proteins termed Exo70p and Exo84p. Loss of function of these proteins in yeast causes accumulation of vesicles destined for the plasma membane[2,4]. The yeast exocyst is localized to sites where active exocytosis and membrane addition take place, and it functions as an effector of Sec4p, a vesicle-associated Rab GTPase[1,3]. The first point of contact between the transport vesicle and the exocyst is through the association of Sec15p with GTP-bound Sec4p. A further interaction between Sec15p and Sec10p is then able to recruit other components of the exocyst and target the vesicles to the specific cell membrane site defined by Sec3p[5]. Therefore, in yeast, Sec15p is believed to link Sec4p and downstream fusion effectors at discrete cellular locations.

The exocyst is evolutionarily conserved from yeast to human. In mammals, it has roles in a variety of tissues. In Madin-Darby canine kidney epithelial cells, the exocyst (named the Sec6–Sec8 complex) localizes to regions of cell-cell contact. In this system, antibodies against Sec8 can specifically block basolateral but not apical vesicle transport, suggesting that the Sec6–Sec8 complex is involved in directing vesicles to the basolateral area of the plasma membrane[6,7]. In adipocytes, the exocyst is thought to have a role in translocating glucose transporters to the cell surface in response to insulin signaling[8]. Finally, in neurons, the Sec6–Sec8 complex is thought to be involved in neurite outgrowth[9]. Although many other homologs of the 23 Sec proteins[4] (such as Sec1p, Sec17p and Sec18p) have been implicated in neurotransmitter release, none of the vertebrate or *Drosophila* exocyst proteins have been shown to function in this process[10–13].

Loss-of-function studies of *sec8* in mouse and *sec5* in *Drosophila* suggest that the exocyst is required for organismal viability[10,12]. In addition, the effects of removing Sec5 in flies show that it is essential for viability of photoreceptors[10]. However, recent work has shown that mutations in *Drosophila sec15* do not cause cell death[13]. Loss of *sec15* in *Drosophila* leads not to any defect in neurite extension but rather to the formation of synapses between inappropriate partners[13]. The loss in synaptic specificity is related to aberrant targeting of cell adhesion and signaling molecules required for neuronal specificity. The findings are consistent with a role for the exocyst in the transport of specific subsets of vesicles, but not with a general role in transport and fusion of vesicles or in neurotransmitter release. Hence, the effect of loss of *Drosophila sec15* is notably different from, and more specific than, the cell lethality and neurite outgrowth defects reported for loss of *sec5*[10]. This raises the possibility that Sec5 may sustain other essential functions in the absence of Sec15, such that different exocyst components have separable functions.

As a first step in understanding the structure-function relationship of Sec15, we have identified a soluble 35-kDa domain comprising nearly the entire C-terminal half of *Drosophila* Sec15. We provide evidence that this domain (hereafter called the C-terminal domain) is involved in binding some Rab GTPases. We have also determined the crystal structure of the C-terminal domain at 2.5-Å resolution and

[1]Verna and Marrs McLean Department of Biochemistry and Molecular Biology and [2]Program in Developmental Biology, Baylor College of Medicine, Houston, Texas 77030, USA. [3]Laboratory for Molecular Cell Biology, Medical Research Council, University College London, London WC1E 6BT, UK. [4]Departments of Molecular Human Genetics and of Neuroscience and [5]Howard Hughes Medical Institute, Baylor College of Medicine. Correspondence should be addressed to F.A.Q. (faq@bcm.tmc.edu).

Received 17 June; accepted 3 August; published online 11 September 2005; doi:10.1038/nsmb987

pinpointed the Rab-binding site. We have further investigated the functional consequences of the interaction of Sec15 and Rab11 *in vivo*.

RESULTS

Binding of the Sec15 C-terminal domain to Rab11

Recent evidence has shown that Sec15 is an effector for the Rab11 GTPase in mammalian cells[14]. Sec15 colocalizes with Rab11 in the recycling endosome and binds Rab11 in a GTP-dependent manner. However, Sec15 does not bind Rab4, Rab6 or Rab7, which are markers for early endosomes, Golgi, and late endosomes and lysosomes, respectively. To further investigate the binding specificity between *Drosophila* Rab11 and Sec15, we determined the approximate location of the Rab-binding site of *Drosophila* Sec15. Two fragments, the N-terminal half (residues 1–380) with His and Nus tags and the C-terminal half (residues 382–764) with a glutathione *S*-transferase (GST) tag, were expressed in *Escherichia coli* and tested using an *in vitro* binding assay. The C-terminal half but not the N-terminal half binds to native Rab11 preloaded with GTPγS-Mg^{2+} (**Fig. 1a**).

We sought a stable fragment or domain of Sec15 that could be used for further investigation of the Rab binding specificity (**Fig. 1**) and for X-ray structure analysis. A BLAST Conserved Domain Database (CDD)[15] search had previously predicted a putative C-terminal segment (named Sec15 domain in the database) from residues 427 to 763 (**Supplementary Fig. 1** online), but this domain could only be overexpressed in the form of inclusion bodies. To obtain a soluble domain and thereby delineate a folded domain, we designed and tested several constructs, but only one construct, containing residues 382–699 (35 kDa), yielded the desired fragment. We named this construct the Sec15 C-terminal domain. Though it is slightly shorter than the entire C-terminal half of Sec15, it binds Rab to a comparable extent (**Fig. 1a**). The mammalian Sec15 binds only to native Rab11 loaded with GTP analog or to its Q70L mutant, which is locked in the GTP-bound conformation[14]. We therefore determined whether the *Drosophila* Sec15 C-terminal domain has the same feature. We used GST derivatives of various forms of *Drosophila* Rab11, including the full-length GTP-restricted Rab11 Q70L mutant and its C-terminal truncation mutant (containing residues 1–200, with 14 C-terminal residues deleted), the full-length Rab11 S25N (a GDP-restricted mutant) and the nucleotide-free Rab11 (**Supplementary Methods** online). There is essentially no binding of the C-terminal domain to the nucleotide-free Rab11 (**Fig. 1b**). In contrast, we observed comparable binding of the C-terminal domain to the full-length Rab11 Q70L and its truncation mutant. As expected, the full-length GDP-restricted mutant Rab11 S25N binds considerably less efficiently than does the full-length GTP-restricted mutant Rab11 Q70L. This is consistent with the yeast two-hybrid results obtained for the binding of the full-length mammalian Sec15[14]. Thus, the *Drosophila* Sec15 C-terminal domain and the full-length mammalian Sec15 share very similar binding efficiencies for Rab11 *in vitro*.

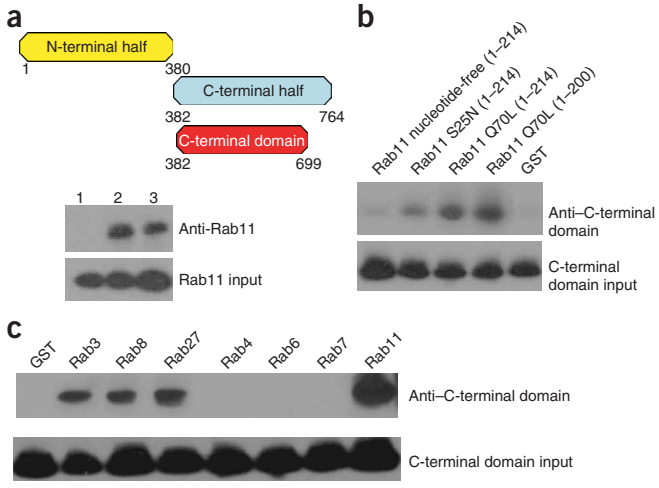

Figure 1 Results of *in vitro* binding assays to test the interactions of the *Drosophila* Sec15 C-terminal domain with Rab GTPases. (**a**) Demonstration that the C-terminal domain contains the Rab-binding site. Above, schematic showing the N-terminal half of Sec15 (1), the C-terminal half (2) and the C-terminal domain (3) (numbers denote residues spanned by each region). Below, western blots with anti-Rab11 after incubation of each of these proteins with GTPγS-Mg^{2+}-Rab11, measuring binding to Rab11. The bottom panel shows the total Rab11 input. (**b**) Results of *in vitro* binding assays to determine the interactions between the C-terminal domain and various forms of GST-Rab 11. Each of the GST-Rab proteins was incubated with the C-terminal domain, pulled down with glutathione–Sepharose beads and probed by Sec15 antibodies. The bottom panel shows the C-terminal input. (**c**) Detection of the binding of the C-terminal domain to other Rabs, all preloaded with GTPγS-Mg^{2+}, as in **b**.

Sec15 affects Rab11 localization *in vivo*

Having shown that the Sec15 C-terminal domain binds to Rab11 in a GTP-dependent manner, we proceeded to examine the functional implications of this interaction in fly photoreceptors. Rab11 has a role in the delivery of rhodopsin-containing vesicles in photoreceptors[16,17]; we therefore chose to examine Rab11 in developing *sec15*-mutant photoreceptors (**Fig. 2**). The *Drosophila* compound eye is composed of hundreds of repeating single eyes called ommatidia, each with its own lens and complement of eight photoreceptor cells. Rhodopsin is deposited in cellular structures called rhabdomeres, which are functionally analogous to the rod outer segments of vertebrate photoreceptors. During development, the rhabdomeres form at the center of the ommatidium, where the photoreceptors make apical cell junctions with each other[18]. Sec15 is enriched in the developing rhabdomeres (**Fig. 2a**), where it partially colocalizes with Rab11 (**Fig. 2b,c**), which appears in punctae in and around the rhabdomeres (**Fig. 2d–f**). Compared to developing wild-type ommatidia, *sec15*-mutant ommatidia showed strong accumulations of Rab11 within the photoreceptors' apical membranes (the location of the rhabdomeres; **Fig. 2g–l**). Analysis of neighboring wild-type and *sec15*-mutant ommatidia showed that the Rab11 accumulation in the mutant tissue was limited to the center of the ommatidia, where rhabdomeres form (**Fig. 2m–o**), and that Rab11 was upregulated in the mutant tissue (**Fig 2n**, arrow). We conclude from these data that Sec15 is required for the normal trafficking of Rab11 and that in the absence of Sec15, Rab11 accumulates at its target membrane. This may explain why adult *sec15*-mutant photoreceptors have rhabdomeres that are shorter than those of the wild type (**Fig. 3a–f**). In agreement with these data, *sec15*-mutant ommatidia have a normal complement of photoreceptors, but the rhabdomeres are smaller than wild-type (**Fig. 3g**). However, as mutant photoreceptors age, some rhabdomeres fuse (data not shown).

C-terminal domain also binds Rab3, Rab8 and Rab27

Previous studies in yeast have shown that Sec15 is an effector of Sec4p, a vesicle-associated Rab GTPase[3]. At least 29 Rab proteins have been described thus far in *Drosophila*. They most likely have roles in different steps of the secretory pathway, but none of these have been reported to be equivalent to the yeast Sec4p[19,20].

Although we present evidence that in *Drosophila* Sec15 is an effector of Rab11, three other exocytic Rab proteins (Rab3, Rab8 and Rab27)

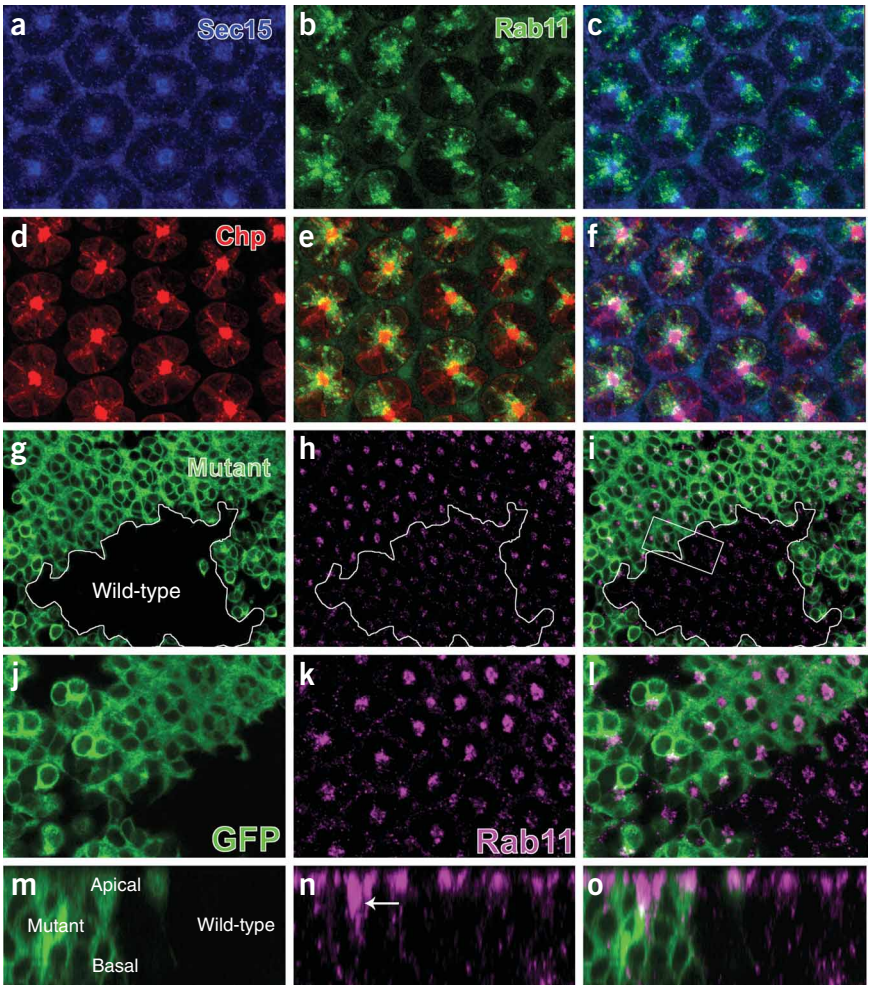

Figure 2 Rab11 is upregulated in *sec15*-mutant tissue and colocalizes with Sec15. (**a**–**f**) Eye from a control 55% pupa. (**a**) Sec15 staining (blue). (**b**) Localization of a Rab11-GFP fusion protein (green) from a genomic construct that can rescue Rab11 mutations[46]. (**c**) Sec15 and Rab11 channels merged. At the rhabdomeres, punctae of Rab11 colocalize with Sec15. (**d**) Chaoptin staining (red), which marks photoreceptor cell membranes. The strong chaoptin staining at the center of the ommatidia marks the location of rhabdomeres. (**e**) Rab11 and chaoptin channels merged. Yellow punctae at the center of the ommatidia indicate where Rab11 makes contact with the rhabdomeres. (**f**) All three channels merged. (**g**–**o**) *sec15*-mutant mosaic eye from a 40% pupa. (**g**) *sec15*-mutant tissue marked by CD8-GFP expression (green). White border indicates a wild-type clone. (**h**) Rab11 immunoreactivity (purple). In *sec15*-mutant tissue, there are increased levels of Rab11 at the center of each ommatidium, where rhabdomeres are forming. (**i**) Both Rab11 staining and GFP expression. (**j**–**l**) Enlargements of the images in **g**–**i**, delineated by white box border in **i**. (**m**–**o**) Tissue samples used in **g**–**l**, a *sec15*-mutant ommatidium and its wild-type neighbor, visualized in the saggital plane to examine the apical-basal distribution of Rab11. (**m**) Orientation of the ommatidia, with GFP expression (green) indicating the *sec15*-mutant ommatidium. (**n**) Rab11 immunoreactivity (purple, as in **h**). Rab11 staining accumulates at the center of the ommatidium in the *sec15*-mutant tissue, as indicated by the arrow. (**o**) Merged images of **m** and **n**.

are potential Sec4 homologs in flies[21]. Rab3 is the most abundant synaptic vesicle–associated Rab[22–24], and *Caenorhabditis elegans* Rab3 null mutants have a reduced number of vesicles at active zones[25], suggesting a targeting defect. The Rab27 subfamily is most similar to the Rab3 subfamily. In addition, Rab27 and Rab3 are often associated in exocytotic vesicles in some secretory cells[26,27]. However, Rab27 seems to have a more specific role in the movement of melanosomes and in granule release in cytotoxic T lymphocytes[28–31]. Finally, Rab8 is among the *Drosophila* sequences most similar to Sec4p (58% identity and 79% similarity), and vertebrate Rab8 seems to selectively regulate basolateral transport in polarized Madin-Darby canine kidney cells[32], a process in which the Sec6–Sec8 complex has also been implicated[6,7].

To investigate whether the C-terminal domain binds Rab3, Rab8 and Rab27 as well as Rab4, Rab6 and Rab7, we used the GST-tagged Rab proteins in binding assays (**Supplementary Methods**). The results show that the C-terminal domain binds Rab3, Rab8 and Rab27 but not Rab4, Rab6 or Rab7 (**Fig. 1c**), suggesting that Sec15 could be an effector of Rab3, Rab8 and Rab27 as well. The failure of the C-terminal domain to bind Rab4, Rab6 and Rab7 is in agreement with previous data showing that the full-length mammalian Sec15 does not interact with the same three Rabs[14].

A novel structure of the C-terminal domain

The crystal structure of the C-terminal domain, determined by MAD phasing from a selenomethionine (SeMet) derivative (**Table 1**), is elongated (~3:1 axial ratio) and composed of two subdomains (**Fig. 4a**), named the N-terminal (N) subdomain (residues 382–563) and C-terminal (C) subdomain (residues 564–699).

The structure is comprised entirely of α-helices (**Fig. 4a**), a total of ten, which are equally distributed between the two subdomains. Whereas the lengths of the five helices in the N subdomain (α1–5) vary considerably (10–32 residues), the helices in the C subdomain (α6–10) have essentially the same length (18–21 residues; **Supplementary Fig. 1**). Moreover, the geometrical arrangements of the helices in the two subdomains differ (**Fig. 4a**). In the N subdomain, the last three α-helices (α3, α4 and α5) form a triple-stranded antiparallel coiled-coil bundle. The first helix (α1), the longest in the domain structure, packs slightly diagonally against the bundle and is linked to α3 by a long (~30 residues), meandering loop punctuated by the shortest helix (α2). Helix α5 is followed by a 20-residue loop that eventually connects to α6 of the C subdomain. A 7-residue segment in the beginning of the loop was missing in the electron density maps, indicating flexibility. Compared to the N subdomain, the C subdomain is more compact, largely because all of its five antiparallel helices form a helix bundle and the loops connecting the helices are relatively short.

The end-to-end stacking of the two subdomains, which generates the elongated structure of the C-terminal domain, is not strong, burying only about 900 Å^2 of accessible surface area. Moreover, although a total of 17 residues, mostly hydrophobic, occupy the

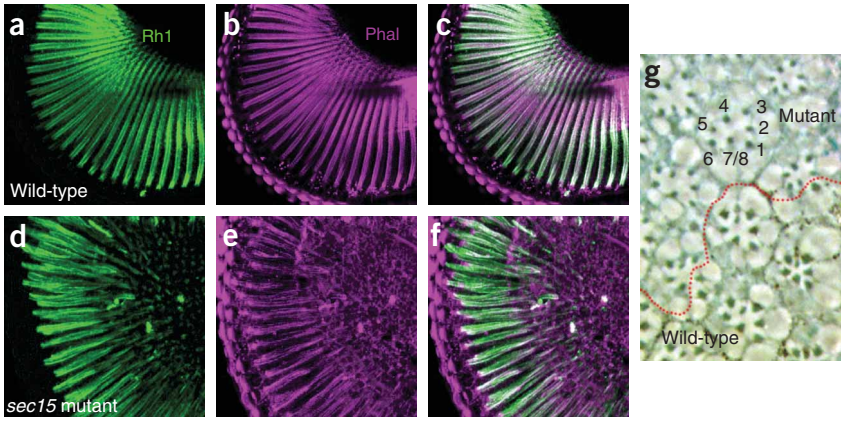

Figure 3 *sec15*-mutant photoreceptors have a defect in a Rab11-dependent process. (**a**–**c**) Section of a control adult eye expressing Rh1-GFP. (**a**) Rhodopsin1 staining. The long tube-like structures are rhabdomeres. (**b**) Phalloidin immunostaining marks actin-rich structures such as the rhabdomeres. (**c**) Rh1Ab staining and phalloidin channels merged. All rhodopsin1 staining is contained within the rhabdomeres, which extend through the length of the eye. (**d**–**f**) Section of a *eyflp sec15*-mutant adult eye expressing Rh1-GFP. (**d**) Rhodopsin1 channels. (**e**) Phalloidin channels. (**f**) Merged images of **d** and **e**. *sec15*-mutant rhabdomeres are shorter than control, and most or all of the rhodopsin is still contained within the rhabdomeres. (**g**) Unstained epoxy section of an adult *sec15*-mutant mosaic eye. The normal complement of photoreceptors is visible in mutant ommatidia. The diameter of the rhabdomeres is reduced.

interface between the two subdomains (**Supplementary Fig. 2** online), only a few of them make intersubdomain van der Waals contacts. There is, however, an unusual web of hydrogen bonds at the interface, with the almost completely buried Arg572 in the C subdomain serving as the focal point for a noncovalent link between the two subdomains (**Supplementary Fig. 2**). Each of three different NH groups of the guanidinium donates a hydrogen bond to a different main chain carboxyl oxygen (two from the N subdomain and one from the C subdomain). The formal positive charge of the arginine side chain is therefore compensated by the partial negative charges of the dipolar carbonyl oxygens, a process called 'ion-dipole interaction' that has been observed previously not only in the interactions of charged residues but also in the binding of ions in proteins[33]. To determine whether this ion-dipole interaction is relevant to the interaction of the C-terminal domain with Rab11, Arg572 was mutated to alanine to disrupt the network and possibly perturb the intersubdomain geometry. The mutation had no deleterious effect on the interaction (**Fig. 4b** and **Supplementary Table 1** online). This result offers the first hint that binding of the C-terminal domain to Rabs may not require both subdomains.

A single helix interacts mainly with Rab11

We sought further molecular understanding of the Sec15-Rab interaction by determining which of the subdomains is involved in binding, by performing site-directed mutagenesis experiments to locate the site for binding and by taking into account the wealth of information on this type of binding in crystal structures of complexes of effectors and their GTPases. The structures of at least ten complexes have been reported, each of which requires only one domain of the effector. Of these structures, five involve effector domains with essentially all helical motifs, including those of arfaptin2, protein kinase N (PKN) ACC finger, N-GAT, GRIP and rabphilin-3A[34]. Further comparison of the five GTPase–helical effector complexes revealed three prominent common features. (i) Helices (a pair of antiparallel helices in the first four effectors and one helix in rabphilin-3A) are important in binding. (ii) Although the helices have no consensus sequence for binding, they interact with nonpolar patches in the so-called 'switch 1 and 2' regions of their cognate GTPases. In those effectors requiring a pair of antiparallel helices, one helix interacts mainly with one switch region while the second helix contacts mainly the other switch region.

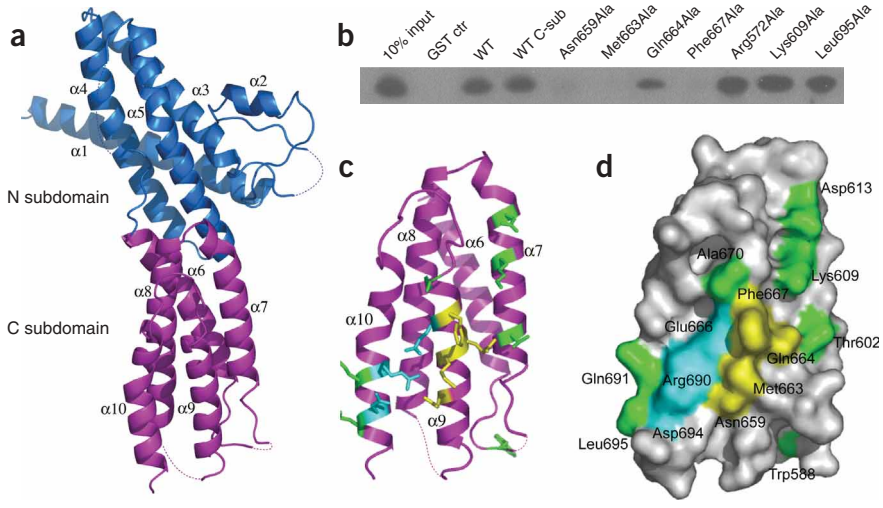

Figure 4 Crystal structure of the Sec15 C-terminal domain and mapping of Rab11 binding sites by mutagenesis. (**a**) Ribbon backbone trace. Blue and magenta, the N and C subdomains, respectively; dashed lines, missing loops. (**b**) Results of *in vitro* assay of the binding of the C subdomain and various C-terminal domain mutants to Rab11. GST-tagged Rab11 Q70L was incubated with wild-type C subdomain (WT C-sub) or C-terminal domain mutants, pulled down with glutathione–Sepharose beads and detected by staining with Sec15 antibody. Lane 1, 10% of input of purified C-terminal domain. The wild-type C-terminal domain (WT) served as a reference and GST alone served as a control. (**c**) Structure of only the C subdomain of the C-terminal domain, showing selected residues subjected to site-directed mutagenesis (complete data in **Supplementary Table 1**). The residues are on a face of the subdomain made up of α7, α9 and α10. Behind this face is another face composed of α6 and α8. Yellow, residues identified as participating in Rab11 binding; green, residues that were mutated but do not affect binding; cyan, three residues (Arg690 and Asp694 from α10 and Glu666 from α9) that form a network of salt links. Residue labels are omitted for clarity but shown in **d**. (**d**) Surface representation of structure in **c** with identical color key. **a**, **b** and **d** were drawn with PyMOL (http://www.pymol.org).

However, there is no one common pattern for the pairing between helices and switch regions. The one helix in rabphilin-3A interacts primarily with switch 1. A more distant variant is the complex between Rab5 and rabaptin5, where a helical segment of the effector forms a dimer, but Rab5 nevertheless still uses its switch regions to contact two helices, one from each unit of the dimer[35]. (iii) Mostly nonpolar residues within the helices interact with the switch regions.

As the two subdomains of the Sec15 C-terminal domain have no structural homology to the other all-helical effector domains, we first investigated whether only one subdomain is engaged in binding Rab11. Several constructs of each subdomain were prepared, but only the C subdomain (residues 565–764) with an N-terminal intein–chitin binding domain (CBD) tag was soluble (**Supplementary Methods**). Fortunately, the intein-CBD–tagged C subdomain bound the GTP-restricted Rab11 Q70L as well as the His-tagged C-terminal domain (**Fig. 4b**), showing that the C subdomain is sufficient for binding.

To determine, by site-directed mutagenesis, which residues are important for binding (**Supplementary Methods**), we used the original high-expression construct of the His-tagged C-terminal domain (described above). Several conserved, hydrophobic, solvent-exposed side chains in the C subdomain were initially chosen for replacement by an Ala residue, including Phe580 (α6), Trp588 (part of the invariant Tyr-Asp-Trp motif between α6 and α7), Phe667 (α9) and Leu695 (α10) (**Supplementary Fig. 1** and **Supplementary Table 1**). None of the conserved hydrophobic residues within α7 and α8 were targeted for mutagenesis, as they are mostly buried. We especially focused on the 18-residue α9 because it has the greatest number of conserved residues (eight identical and nine similar residues), compared to the other four helices in the C subdomain (**Supplementary Fig. 1**). Although Phe667 in α9 is not completely conserved, it was chosen for replacement because it is the most exposed (44.3% accessible surface). A complete list of the residues mutated and a summary of data are given in **Supplementary Table 1**, and key results are shown in **Figure 4b–d.** Of the mutations initially introduced, only F667A in α9, located on one side of the surface of the C subdomain, abrogated binding to Rab11 (**Fig. 4b**).

To more narrowly define the Rab11-binding area, we further mutated exposed conserved residues close to and on the same surface location as Phe667, including six other residues in α9 as well as residues in helices α7 and α10 that flank α9 on both sides. Single mutations of α9 residues that are nearly on the same track on the helix as Phe667 (M663A and N659A) essentially abolished binding (**Fig. 4b–d**). Mutation of the invariant α9 residue Gln664, whose side chain points toward the N terminus of α7 (**Fig. 4c,d**), to alanine or glutamate reduced binding to roughly half that observed for the unmodified C-terminal domain (**Fig. 4b**). Replacement of Ala670, located at the C terminus of α9 (**Fig. 4c,d**), by a bulkier and negatively charged glutamate did not affect the C-terminal domain–Rab11 interaction. Thus, the surface area on α9 involved in Rab11 binding extends at least from Asn659 to Phe667, with Met663, Gln664 and possibly Leu660, which is slightly exposed, making up the intervening residues.

Single mutations of conserved residues within α7 (D613A and T602E at the C and N termini, respectively, and Lys609 at midpoint of the helix) had no effect on binding by the C-terminal domain (**Fig. 4b–d**). This finding, together with the observation of only a small reduction in binding associated with the mutation of Gln664, whose side chain abuts α7 as described above, indicates that α7 is not involved in the interaction with Rab11.

Although α10 is antiparallel to α9, it does not have the features associated with binding to Rabs, as its most exposed conserved residues are highly polar (Arg690, Gln691 and Asp694). The invariant Arg690 is of particular interest because it is the closest to the functional segment of α9 (**Fig. 4c,d**). However, the guanidinium group of Arg690 is tied up by two salt links with Glu666 of α9 and Asp694 of α10 (**Fig. 4c**), which could preclude its participation in binding. Replacement of each of the three residues involved in the salt links by alanine resulted in an insoluble domain. Additional single mutations of α10 residues Gln691 and Leu695, whose side chains are very much exposed but nowhere near α9 (**Fig. 4c,d**), to alanine did not affect binding.

Because rabphilin-3A uses one helix for binding Rab3[34,36], we used the structure of this complex as a template to model the interaction of the Sec15 C subdomain with Rab11. Helix α9 (residues 658–670) of the C subdomain was aligned to the helical binding region (residues 50–62) of rabphilin-3A, and the crystal structure of Rab11 with bound GTP analog[37] was in turn superimposed on the Rab3 structure (**Supplementary Fig. 3** online). The modeling showed that the set of functional residues in the C subdomain are close to the switch regions of Rab11 (**Supplementary Fig. 3**).

DISCUSSION

Sec15 plays multiple key roles in a variety of processes in exocytosis by interacting with vesicle-associated small Rab GTPases, assisting in targeting vesicles to budding sites and recruiting, by way of Sec10, other components of the exocyst. Our *in vitro* and *in vivo* studies have shed light on some of these roles.

The relatively large size (85 kDa) of Sec15 ensures that there are enough docking sites, each probably residing in either a single domain or a combination of domains, for other protein components necessary for its diverse functions. Our studies revealed a segment named the C-terminal domain, containing nearly the entire C-terminal half of the protein, with several interesting properties. This domain binds to a set of Rabs in a GTP-dependent manner. Its atomic structure is composed of two distinct subdomains, only one of which (the C subdomain) harbors the Rab-binding site. The finding of a bipartite C-terminal domain was unexpected, as there was no hint of this feature even from the BLAST CDD[15] search for domains. The all-helical structure of the domain (**Fig. 4a**), with its two different subdomains, has a novel fold. A search for overall structural similarities of the whole domain and of the N and C subdomains separately against the DALI[38] database did not find any substantial matches.

Our binding studies further show that Sec15 lacks stringent substrate specificity *in vitro*. The domain binds Rab11, Rab3, Rab8 and Rab27, but the binding data (**Fig. 1c**) suggest that Rab11 is the major target. The ability of an effector protein to interact with different Rab proteins has been observed previously: rabphilin-3, originally identified as a Rab3-binding protein, has also been shown to interact with Rab8 and Rab27 in a cotransfection assay in COS-7 cells[39]. In addition, Sec15 and Sec5 apparently do not have a significant role in regulating neurotransmitter release[10,13], a process in which Rab3 has been implicated. This suggests that the weaker *in vitro* binding of Sec15 with Rab3, Rab8 and Rab27 may have *in vivo* consequences. It remains to be investigated whether these interactions have any role *in vivo*.

The Rab-binding site is apparently confined mainly to the exposed middle three-fourths of one helix (α9) of the C subdomain, which contains mostly hydrophobic residues (**Fig. 4c,d**). The participation of hydrophobic residues in binding is a common feature observed in several crystal structures of complexes of effectors with their cognate small GTPases[34]. The *in vivo* consequence of abolishing the Sec15-Rab11 interaction by using the Sec15 mutants is under investigation.

Table 1 Crystallographic statistics

	Native	SeMet MAD		
Data collection				
Space group	$C222_1$		$C222_1$	
Cell dimensions				
a, *b*, *c* (Å)	80.80, 94.35, 123.31		83.50, 94.93, 123.47	
α, β, γ (°)	90, 90, 90		90, 90, 90	
		Peak	*Inflection*	*Remote*
Wavelength	0.933	0.97958	0.97949	0.96308
Resolution (Å)	50–2.5	50–3.0	50–3.0	50–3.0
R_{sym}[a]	5.5 (37.5)	6.8 (56.1)	6.6 (56.8)	6.6 (56.2)
$I/\sigma I$[a]	40.4 (3.5)	32.5 (2.5)	32.0 (2.4)	31.5 (2.5)
Completeness (%)[a]	98.5 (96.7)	99.9 (99.2)	99.8 (98.6)	99.8 (99.3)
Redundancy[a]	7.1 (6.0)	6.4 (5.9)	6.4 (5.9)	6.4 (6.0)
Refinement				
Resolution	50–2.5			
No. of reflections[b]	113,932			
R_{work} / R_{free}	0.243 / 0.276			
No. of atoms				
Protein	2,425			
Water	87			
B-factors				
Protein	67.3			
Water	75.8			
R.m.s. deviations				
Bond lengths (Å)	0.01			
Bond angles (°)	1.26			

[a]Highest-resolution shell is shown in parentheses. [b]Reflections $|F_{obs}| > 1.0\ \sigma$.

Our studies further raise questions about the role of the ~15-kDa N subdomain, which is also composed entirely of helices, but helices with various lengths and with topology and geometry different from those in the C subdomain. The same questions could also apply to the function(s) of the ~40-kDa N-terminal half of Sec15. The combination of the N subdomain and the N-terminal half, which is approximately two-thirds of the entire Sec15 protein, seems too large for binding only the Sec10 component of the exocyst. This suggests that Sec15 may have additional partners that have yet to be identified.

There are informative differences between the phenotypes in rhodopsin1 trafficking and rhabdomere morphogenesis of *rab11* and *sec15* mutants. A defect in the initial delivery of rhodopsin in *rab11* mutants has been associated with accumulations of rhodopsin outside the rhabdomere[17]. We did not observe noticeable amounts of rhodopsin outside the rhabdomeres in *sec15* mutants (**Figs. 3d–f**). This observation, combined with the normal photoreceptor depolarization measured by electroretinography[13], suggests that initial delivery of rhodopsin occurs in *sec15* mutants. However, there is also a significant defect in rhabdomere morphology in *rab11* mutant photoreceptors[17]. Hence, our photoreceptor staining data (**Fig. 3d–f**) suggest that although targeted membrane delivery to the rhabdomere might occur in Sec15-mutant cells, defects in membrane recycling (evidenced by the strong accumulation of Rab11 in the rhabdomere) probably lead to disruptions in rhabdomere morphology over time. Together, these data suggest that the *rab11* mutant phenotype is more severe than the *sec15* mutant phenotype but that the two show some similarities. In summary, the interaction of Rab11 and Sec15 has functional consequences *in vivo*, in that Rab11 trafficking is disrupted in *sec15* mutants and at least one aspect of the *sec15* mutant phenotype, namely abnormal rhabdomere morphology, can be explained by loss of Rab11 function. An interaction between Sec15 and Rab11 has recently also been shown to have an important role in the asymmetric division of sensory organ precursors in *Drosophila*[40], suggesting that their interaction is required not only in rhodopsin targeting but also during cell-fate specification.

METHODS

Expression, purification and crystallization. The DNA sequence corresponding to the Sec15 C-terminal domain was amplified by PCR and cloned into the pET-21b expression vector (Novagen) with a 6× His tag at the C terminus. The protein was expressed in *E. coli* Rosetta cells (Novagen), and cells were broken by French press and the protein purified to near homogeneity using Talon Co^{2+} metal affinity beads (BD Biosciences). To remove minor impurities, the protein was subjected to chromatography on a MonoQ column and the stock protein solution was concentrated in 20 mM NaCl and 20 mM Tris (pH 8.0). The protein was crystallized at room temperature using hanging drop vapor diffusion, with the drop consisting of a 1:1 mixture of the stock protein solution and the reservoir solution of 100 mM sodium citrate and 200 mM $NH_4H_2PO_4$ (pH 5.6). Rod-like crystals of dimensions up to 0.3 × 0.15 × 0.1 mm appeared within one week.

Structure determination. The structure of the C-terminal domain was determined by MAD. A MAD data set was collected from a crystal of the SeMet variant of the C-terminal domain on beamline 8.2.1 at Advanced Light Source, Lawrence Berkeley National Laboratory, Berkeley, California, USA. Data were processed and merged with HKL2000[41]. The positions of 10 out of a total of 12 SeMet sites were found using CNS[42]. Heavy atom parameters were refined, MAD phases were calculated to 3-Å resolution with the figure of merit 0.68 and the electron density map was solvent-flattened using the SHARP suite[43]. Model building and refinement were done with O[44] and CNS[42]. Crystallographic statistics are summarized in **Table 1**.

***In vitro* assay to test binding of Sec15 to Rab11.** Full-length Rab11 (residues 1–214) was cloned into the pTYB12 expression vector (New England Biolabs) as an N-terminal intein-CBD fusion protein. The GTPγS loading reaction was carried out by incubating purified Rab11 with 1 mM GTPγS and 5 mM EDTA in PBS (pH 7.4) for 20 min at 37 °C, and the reaction was terminated by adding 10 mM $MgCl_2$. The N-terminal half of Sec15 (residues 1–380) was cloned into pET-43.1 EK/LIC (Novagen) as a Nus-His fusion protein. The C-terminal half of Sec15 (residues 382–764) was cloned into the pGEX-4T-1 (Amersham Biosciences) vector as a GST fusion protein. The C-terminal domain was purified as described above. Each of the three recombinant Sec15 fragments was loaded onto Talon beads (for the N-terminal half and C-terminal domain) or glutathione beads (for the C-terminal half) and washed extensively. 50 µl Talon or glutathione beads with ~2 nmol of bound Sec15 fragment were incubated with Rab11-GTPγS (~5 nmol) in PBS solution supplemented with 2 mM DTT, 10 mM $MgCl_2$ (solution A) at 4 °C for 1 h. Each incubation mixture was then pelleted by centrifugation for 30 s at 2,000*g* and washed three times with 1 ml of solution A with 0.1% (v/v) IGEPAL detergent (solution B). The proteins bound to the beads were released by boiling in SDS loading buffer and analyzed by SDS-PAGE, and immunoblots were probed with antibodies to Rab11 (anti-Rab11).

Immunohistochemistry. Larval and pupal eyes were fixed in PBS with 3.5% (v/v) formaldehyde for 15 min and washed in PBS with 0.4% (v/v) Triton

X-100. Antibody dilutions were as follows: anti-Sec15 1:2,000 (ref. 13); mAb24B10 (anti-chaoptin) 1:50 (ref. 45); anti-Rab11 1:2,000 (ref. 46); and mAb4C5 (anti-Rh1) 1:50 (University of Iowa Developmental Studies Hybridoma Bank, Iowa City, Iowa, USA). Phalloidin–Texas red was used to mark the F-actin–rich rhabdomeres (**Fig. 3**). *Drosophila* strains, conditions of culture and image acquisition and processing are described in **Supplementary Methods**.

Accession codes. Protein Data Bank: Coordinates have been deposited with accession code 2A2F. BIND identifiers (http://bind.ca): 316309–316312.

Note: Supplementary information is available on the Nature Structural & Molecular Biology website.

ACKNOWLEDGMENTS

We thank the staff at Lawrence Berkeley National Laboratory beamline 8.2.1 for their help with the X-ray data collection. We thank J. He and J.L. Fallon for their technical assistance and R. Cohen (University of Kansas, Lawrence, Kansas, USA) for the Rab11 antibody, Rab11-GFP line and Rab11 mutants. S.W. was supported in part by a training fellowship from the W.M. Keck Foundation to the Gulf Coast Consortia through the Keck Center for Computational and Structural Biology and by a grant from the Welch Foundation (Q-0581) to F.A.Q. S.Q.M. was supported by the US National Institutes of Health grant EY07001 and is a member of the Medical Scientist Training Program. A significant part of the work in the laboratories of F.A.Q. and H.J.B. was supported by the Howard Hughes Medical Institute. Work in F.P.'s laboratory was supported by the Medical Research Council and the Biotechnology and Biological Sciences Research Council.

COMPETING INTERESTS STATEMENT

The authors declare that they have no competing financial interests.

Published online at http://www.nature.com/nsmb/
Reprints and permissions information is available online at http://npg.nature.com/reprintsandpermissions/

1. TerBush, D.R. & Novick, P. Sec6, Sec8, and Sec15 are components of a multisubunit complex which localizes to small bud tips in *Saccharomyces cerevisiae*. *J. Cell Biol.* **130**, 299–312 (1995).
2. TerBush, D., Maurice, T., Roth, D. & Novick, P. The exocyst is a multiprotein complex required for exocytosis in *Saccharomyces cerevisiae*. *EMBO J.* **15**, 6483–6494 (1996).
3. Guo, W., Roth, D., Walch-Solimena, C. & Novick, P. The exocyst is an effector for Sec4p, targeting secretory vesicles to sites of exocytosis. *EMBO J.* **18**, 1071–1080 (1999).
4. Novick, P., Field, C. & Schekman, R. Identification of 23 complementation groups required for post-translational events in the yeast secretory pathway. *Cell* **21**, 205–215 (1980).
5. Finger, F.P., Hughes, T.E. & Novick, P. Sec3p is a spatial landmark for polarized secretion in budding yeast. *Cell* **92**, 559–571 (1998).
6. Grindstaff, K.K. *et al.* Sec6/8 complex is recruited to cell-cell contacts and specifies transport vesicle delivery to the basal-lateral membrane in epithelial cells. *Cell* **93**, 731–740 (1998).
7. Yeaman, C., Grindstaff, K.K. & Nelson, W.J. Mechanism of recruiting Sec6/8 (exocyst) complex to the apical junctional complex during polarization of epithelial cells. *J. Cell Sci.* **117**, 559–570 (2004).
8. Inoue, M., Chang, L., Hwang, J., Chiang, S.H. & Saltiel, A.R. The exocyst complex is required for targeting of Glut4 to the plasma membrane by insulin. *Nature* **422**, 629–633 (2003).
9. Vega, I.E. & Hsu, S.-C. The exocyst complex associates with microtubules to mediate vesicle targeting and neurite outgrowth. *J. Neurosci.* **21**, 3839–3848 (2001).
10. Murthy, M., Garza, D., Scheller, R.H. & Schwarz, T.L. Mutations in the exocyst component Sec5 disrupt neuronal membrane traffic, but neurotransmitter release persists. *Neuron* **37**, 433–447 (2003).
11. Bennett, M.K. & Scheller, R.H. The molecular machinery for secretion is conserved from yeast to neurons. *Proc. Natl. Acad. Sci. USA* **90**, 2559–2563 (1993).
12. Friedrich, G.A., Hildebrand, J.D. & Soriano, P. The secretory protein Sec8 is required for paraxial mesoderm formation in the mouse. *Dev. Biol.* **192**, 364–374 (1997).
13. Mehta, S.Q. *et al.* Mutations in *Drosophila* sec15 reveal a function in neuronal targeting for a subset of exocyst components. *Neuron* **46**, 219–232 (2005).
14. Zhang, X.M., Ellis, S., Sriratana, A., Mitchell, C.A. & Rowe, T. Sec15 is an effector for the Rab11 GTPase in mammalian cells. *J. Biol. Chem.* **279**, 43027–43034 (2004).
15. Marchler-Bauer, A. *et al.* CDD: a curated Entrez database of conserved domain alignments. *Nucleic Acids Res.* **31**, 383–387 (2003).
16. Deretic, D. Rab proteins and post-Golgi trafficking of rhodopsin in photoreceptor cells. *Electrophoresis* **18**, 2537–2541 (1997).
17. Satoh, A.K., O'Tousa, J.E., Ozaki, K. & Ready, D.F. Rab11 mediates post-Golgi trafficking of rhodopsin to the photosensitive apical membrane of *Drosophila* photoreceptors. *Development* **132**, 1487–1497 (2005).
18. Wolff, T. & Ready, D.F. Pattern formation in the *Drosophila* retina. in *The Development of Drosophila melanogaster* Vol. II (eds. Bate, M. & Martinez-Arias, A.) 1277–1325 (Cold Spring Harbor Laboratory Press, Cold Spring Harbor, New York, USA, 1993).
19. Segev, N. Ypt and Rab GTPases: insight into functions through novel interactions. *Curr. Opin. Cell Biol.* **13**, 500–511 (2001).
20. Pereira-Leal, J.B. & Seabra, M.C. Evolution of the Rab family of small GTP-binding proteins. *J. Mol. Biol.* **313**, 889–901 (2001).
21. Lloyd, T.E. *et al.* A genome-wide search for synaptic vesicle cycle proteins in *Drosophila*. *Neuron* **26**, 45–50 (2000).
22. Fischer von Mollard, G. *et al.* rab3 is a small GTP-binding protein exclusively localized to synaptic vesicles. *Proc. Natl. Acad. Sci. USA* **87**, 1988–1992 (1990).
23. Stahl, B., Chou, J.H., Li, C., Sudhof, T.C. & Jahn, R. Rab3 reversibly recruits rabphilin to synaptic vesicles by a mechanism analogous to raf recruitment by ras. *EMBO J.* **15**, 1799–1809 (1996).
24. Wang, Y., Okamoto, M., Schmitz, F., Hofmann, K. & Sudhof, T.C. Rim is a putative Rab3 effector in regulating synaptic-vesicle fusion. *Nature* **388**, 593–598 (1997).
25. Nonet, M.L. *et al. Caenorhabditis elegans* rab-3 mutant synapses exhibit impaired function and are partially depleted of vesicles. *J. Neurosci.* **17**, 8061–8073 (1997).
26. Regazzi, R. *et al.* Expression, localization and functional role of small GTPases of the Rab3 family in insulin-secreting cells. *J. Cell Sci.* **109**, 2265–2273 (1996).
27. Yi, Z. *et al.* The Rab27a/granuphilin complex regulates the exocytosis of insulin-containing dense-core granules. *Mol. Cell. Biol.* **22**, 1858–1867 (2002).
28. Araki, K. *et al.* Small Gtpase rab3A is associated with melanosomes in melanoma cells. *Pigment Cell Res.* **13**, 332–336 (2000).
29. Bahadoran, P. *et al.* Rab27a: A key to melanosome transport in human melanocytes. *J. Cell Biol.* **152**, 843–850 (2001).
30. Menasche, G. *et al.* Mutations in RAB27A cause Griscelli syndrome associated with haemophagocytic syndrome. *Nat. Genet.* **25**, 173–176 (2000).
31. Wilson, S.M. *et al.* A mutation in Rab27a causes the vesicle transport defects observed in ashen mice. *Proc. Natl. Acad. Sci. USA* **97**, 7933–7938 (2000).
32. Ang, A.L., Folsch, H., Koivisto, U.M., Pypaert, M. & Mellman, I. The Rab8 GTPase selectively regulates AP-1B-dependent basolateral transport in polarized Madin-Darby canine kidney cells. *J. Cell Biol.* **163**, 339–350 (2003).
33. Vyas, N.K., Vyas, M.N. & Quiocho, F.A. Crystal structure of *M. tuberculosis* ABC phosphate transport receptor: specificity and charge compensation dominated by ion-dipole interactions. *Structure* **11**, 765–774 (2003).
34. Panic, B., Perisic, O., Veprintsev, D.B., Williams, R.L. & Munro, S. Structural basis for Arl1-dependent targeting of homodimeric GRIP domains to the Golgi apparatus. *Mol. Cell* **12**, 863–874 (2003).
35. Zhu, G. *et al.* Structural basis of Rab5-Rabaptin5 interaction in endocytosis. *Nat. Struct. Mol. Biol.* **11**, 975–983 (2004).
36. Ostermeier, C. & Brunger, A.T. Structural basis of Rab effector specificity: crystal structure of the small G protein Rab3A complexed with the effector domain of rabphilin-3A. *Cell* **96**, 363–374 (1999).
37. Pasqualato, S. *et al.* The structural GDP/GTP cycle of Rab11 reveals a novel interface involved in the dynamics of recycling endosomes. *J. Biol. Chem.* **279**, 11480–11488 (2004).
38. Holm, L. & Sander, C. Dali: a network tool for protein structure comparison. *Trends Biochem. Sci.* **20**, 478–480 (1995).
39. Fukuda, M. Distinct Rab binding specificity of Rim1, Rim2, rabphilin, and Noc2. Identification of a critical determinant of Rab3A/Rab27A recognition by Rim2. *J. Biol. Chem.* **278**, 15373–15380 (2003).
40. Jafar-Nejad, H. *et al.* Sec15, a component of the exocyst, promotes Notch signaling during the asymmetric division of *Drosophila* sensory organ precursors. *Dev. Cell* published online 1 Sep 2005.
41. Otwinowski, Z. & Minor, W. Processing of X-ray diffraction data collected in oscillation mode. *Methods Enzymol.* **276**, 307–326 (1997).
42. Brünger, A.T. *et al.* Crystallography & NMR system: a new software suite for macromolecular structure determination. *Acta Crystallogr. D Biol. Crystallogr.* **54**, 905–921 (1998).
43. La Fortelle, E.D. & Bricogne, G. SHARP program for statistical heavy-atom refinement. *Methods Enzymol.* **276**, 472–494 (1997).
44. Jones, T.A., Zou, J.Y., Cowan, S.W. & Kjeldgaard, M. Improved methods for building protein models in electron density maps and the location of errors in these models. *Acta Crystallogr. D Biol. Crystallogr.* **47**, 110–119 (1991).
45. Van Vactor, D., Jr., Krantz, D.E., Reinke, R. & Zipursky, S.L. Analysis of mutants in chaoptin, a photoreceptor cell-specific glycoprotein in *Drosophila*, reveals its role in cellular morphogenesis. *Cell* **52**, 281–290 (1988).
46. Dollar, G., Struckhoff, E., Michaud, J. & Cohen, R.S. Rab11 polarization of the *Drosophila* oocyte: a novel link between membrane trafficking, microtubule organization, and oskar mRNA localization and translation. *Development* **129**, 517–526 (2002).